

Probability & Statistics Note

Note 13

July 2015

EMC/EMI testing requirements optimization using a re-sampling technique – Technical report

Chaouki Kasmi^{1*}, Sébastien Lalléchère², Pierre Bonnet², Sébastien Girard²,
Françoise Paladian², Emmanuel Prouff¹

¹*French Network and Information Security Agency-ANSSI, 51 bvd de la Tour Maubourg, 75007 Paris, France*

²*Université Clermont Auvergne, Université Blaise Pascal, Institut Pascal, CNRS UMR 6602, 63178 Aubière, France*

*chaouki.kasmi@ssi.gouv.fr

Abstract: Recent studies have shown a high interest in statistical methods dedicated to the prediction of the maximum confidence in simulation and measurements for electromagnetic compatibility and electromagnetic interference. In particular, it has been shown that one of the main issues remains the access to a number of samples leading to the estimation of the risks in regards to test set-up random variables. In this paper it is argued that a real-time bootstrapping module enables to optimize the number of experiments while estimating the maximum confidence level of the accessible samples mean contributions.

The authors would like to thank the following scientific contributors to this study:

Dr. Nicolas Mora³ and Prof. Farhad Rachidi³
for hosting Dr. Chaouki Kasmi in February 2013 and organizing the experiments at the EMC
Laboratory of the EPFL dedicated to the analysis of the conducted propagation of
electromagnetic interferences along the low-power network.

³*École Polytechnique Fédérale de Lausanne, EPFL, Lausanne, Suisse*

Prof. Marcos Rubinstein⁴
for the interesting advices concerning the experimental procedures and statistical methods.

⁴*Haute École d'Ingénierie et de Gestion du Canton de Vaud, HEIG-VD, Yverdon, Suisse*

Prof. Marc Hélier⁵ and Dr. Muriel Darces⁵
for their valuable comments concerning the bootstrapping procedure applied to Electromagnetic
Compatibility and Electromagnetic Interference studies.

⁵*Sorbonne Universités, UPMC, Paris 06, UR2, L2E, BC 252, 4 place Jussieu, 75005 Paris, France*

Table of contents

| | | |
|-------|---|----|
| 1. | Introduction: needs for susceptibility testing improvement | 7 |
| 2. | Bootstrapping principle | 8 |
| 3. | Application to EMC/EMI tests | 9 |
| 3.1 | EMC Radiated tests | 9 |
| 3.1.1 | Measurement set-up | 9 |
| 3.1.2 | Classical application | 10 |
| 3.1.3 | Application and validation on mean contributions | 13 |
| 3.1.4 | Application and validation on high quantiles | 14 |
| 3.1.5 | Bootstrap procedure and Central Limit Theorem | 15 |
| 3.2 | Conducted propagation of IEMI along the power network | 17 |
| 3.2.1 | Measurement set-up | 17 |
| 3.2.2 | Conducted propagation of electromagnetic interferences | 17 |
| 3.2.3 | Effects induced by connected electronic devices | 18 |
| 3.2.4 | Analysis of the mean contributions and high quantiles of the induced voltages | 19 |
| 4. | Conclusion | 23 |
| | ANNEX A | 26 |

List of figures

| | |
|--|----|
| Figure 1: Probability density function of a sample S of a population P | 7 |
| Figure 2: Schematic of the accessible set of sample S of a population P | 7 |
| Figure 3: Schematic representation of the implemented algorithms for Monte Carlo process and Bootstrapping method comparison in real-time. | 9 |
| Figure 4: Inner view of the experimental cabinet including external slot, moving plate and internal stirrer [17]. | 10 |
| Figure 5: Schematic representation of the experimental cabinet including external slot, moving plate and internal stirrer [17]. | 10 |
| Figure 6: Mean and standard deviation of three set of random selections of measurement in regards of the length (m) of the samples. | 11 |
| Figure 7: Random selection (8 for graph readability) of samples applying the bootstrap to the received power mean in regards of the length (m) of the selected samples..... | 11 |
| Figure 8: Random selection (8 for graph readability) of samples applying the bootstrap to the received power standard deviation in regards of the length (m) of the selected samples. | 12 |
| Figure 9: Mean (red), standard deviation (green) and confidence interval (black) for the bootstrapped means and 8 random Monte Carlo selections (blue) for illustration purpose in regards of the length (m) of the selected samples. | 13 |
| Figure 10: Mean (red), standard deviation (green) and confidence interval (black) for the bootstrapped standard deviations and 8 random Monte Carlo selections (blue) for illustration purpose in regards of the length (m) of the selected samples. | 13 |
| Figure 11: Standard deviation to mean ratios for MC (blue), bootstrap (red) and related standard deviation confidence interval to mean confidence interval ratios obtained by 1,000 bootstrap replications (black) in regards of the size m of the selected samples..... | 14 |
| Figure 12: Mean (red), standard deviation (green) and maximum confidence interval (black) for the bootstrapped 95th- quantile (Q95) and 8 random Monte Carlo selections (blue) for illustration purpose in regards of the length (m) of the selected samples. | 15 |
| Figure 13: Standard deviation to mean ratios in regards of the length (m) of the selected samples and the number (s) of the bootstrap replications. | 16 |
| Figure 14: Standard deviation to mean ratios of the 1,000 bootstrapped means (red) and of the 1,000 bootstrapped standard deviations (green) in regards of the length (m) of the selected samples. | 16 |
| Figure 15: Electrical raceway under study [22, 23]. | 17 |
| Figure 16: Experimental process in the semi-anechoic chamber at the EMC Laboratory of EPFL [21, 22]. | 18 |
| Figure 17: Experimental process in the semi-anechoic chamber at the EMC Laboratory of EPFL [21, 22]. | 18 |

| | |
|--|----|
| Figure 18: Power transfer function magnitude between the two power sockets AC1-AC3 with the network unloaded and randomly loaded [21, 22]..... | 19 |
| Figure 19: Mean (red), standard deviation (green) and confidence interval (black) for the bootstrapped means and 5 random Monte Carlo selections (blue) for illustration purpose in regards of the length (m) of the selected samples at 4.58 MHz..... | 20 |
| Figure 20: Mean (red), standard deviation (green) and confidence interval (black) for the bootstrapped means and 5 random Monte Carlo selections (blue) for illustration purpose in regards of the length (m) of the selected samples at 160.1 MHz..... | 20 |
| Figure 21: Mean (red), standard deviation (green) and confidence interval (black) for the bootstrapped standard deviations and 5 random Monte Carlo selections (blue) for illustration purpose in regards of the length (m) of the selected samples at 4.58 MHz..... | 21 |
| Figure 22: Mean (red), standard deviation (green) and confidence interval (black) for the bootstrapped standard deviations and 5 random Monte Carlo selections (blue) for illustration purpose in regards of the length (m) of the selected samples at 160.1 MHz..... | 21 |
| Figure 23: Mean (red), standard deviation (green) and maximum confidence interval (black) for the bootstrapped 95th- quantile (Q95) and 5 random Monte Carlo selections (blue) for illustration purpose in regards of the length (m) of the selected samples at 4.58 MHz..... | 22 |
| Figure 24: Mean (red), standard deviation (green) and maximum confidence interval (black) for the bootstrapped 95th- quantile (Q95) and 5 random Monte Carlo selections (blue) for illustration purpose in regards of the length (m) of the selected samples 160.1 MHz..... | 22 |
| Figure 25: Mean (red), standard deviation (green) and confidence interval (black) for the bootstrapped means and 5 random Monte Carlo selections (blue) for illustration purpose in regards of the length (m) of the selected samples at 4.58 MHz..... | 26 |
| Figure 26: Mean (red), standard deviation (green) and confidence interval (black) for the bootstrapped means and 5 random Monte Carlo selections (blue) for illustration purpose in regards of the length (m) of the selected samples at 160.1 MHz..... | 27 |
| Figure 27: Mean (red), standard deviation (green) and confidence interval (black) for the bootstrapped standard deviations and 5 random Monte Carlo selections (blue) for illustration purpose in regards of the length (m) of the selected samples at 4.58 MHz..... | 27 |
| Figure 28: Mean (red), standard deviation (green) and confidence interval (black) for the bootstrapped standard deviations and 5 random Monte Carlo selections (blue) for illustration purpose in regards of the length (m) of the selected samples at 160.1 MHz..... | 28 |
| Figure 29: Mean (red), standard deviation (green) and maximum confidence interval (black) for the bootstrapped 95th- quantile (Q95) and 5 random Monte Carlo selections (blue) for illustration purpose in regards of the length (m) of the selected samples at 4.58 MHz..... | 28 |
| Figure 30: Mean (red), standard deviation (green) and maximum confidence interval (black) for the bootstrapped 95th- quantile (Q95) and 5 random Monte Carlo selections (blue) for illustration purpose in regards of the length (m) of the selected samples at 160.1 MHz..... | 29 |
| Figure 31: Mean (red), standard deviation (green) and confidence interval (black) for the bootstrapped means and 5 random Monte Carlo selections (blue) for illustration purpose in regards of the length (m) of the selected samples at 4.58 MHz..... | 30 |

| | |
|---|----|
| Figure 32: Mean (red), standard deviation (green) and confidence interval (black) for the bootstrapped means and 5 random Monte Carlo selections (blue) for illustration purpose in regards of the length (m) of the selected samples at 160.1 MHz. | 31 |
| Figure 33: Mean (red), standard deviation (green) and confidence interval (black) for the bootstrapped standard deviations and 5 random Monte Carlo selections (blue) for illustration purpose in regards of the length (m) of the selected samples at 4.58 MHz. | 31 |
| Figure 34: Mean (red), standard deviation (green) and confidence interval (black) for the bootstrapped standard deviations and 5 random Monte Carlo selections (blue) for illustration purpose in regards of the length (m) of the selected samples at 160.1 MHz. | 32 |
| Figure 35: Mean (red), standard deviation (green) and maximum confidence interval (black) for the bootstrapped 95th- quantile (Q95) and 5 random Monte Carlo selections (blue) for illustration purpose in regards of the length (m) of the selected samples at 4.58 MHz. | 32 |
| Figure 36: Mean (red), standard deviation (green) and maximum confidence interval (black) for the bootstrapped 95th- quantile (Q95) and 5 random Monte Carlo selections (blue) for illustration purpose in regards of the length (m) of the selected samples at 160.1 MHz. | 33 |

List of tables

| | |
|---|----|
| Table 1: MC results | 11 |
| Table 2: Results for Bootstrap (M=1000) in mW | 12 |
| Table 3: MC results of the induced voltage on AC2 | 19 |
| Table 4: MC results of the induced voltage on AC3 | 26 |
| Table 5: MC results of the induced voltage on AC3 | 30 |

1. Introduction: needs for susceptibility testing improvement

Several studies [1-6] have demonstrated that electronic devices are susceptible to intentional electromagnetic interferences (IEMI). In order to reduce the threat of IEMI to tolerable levels, adequate protective devices can be involved. Their design relies on an accurate estimation of the risk levels which is crucial for critical applications.

Recently, the electromagnetic compatibility (EMC) community has shown a high interest in the estimation of the maximum confidence in simulation and measurement results as it may introduce a significant risk for the safety and security of critical infrastructures. Meanwhile, extreme values theory [7-8] and reliability analysis methods [9-10] have recently been proposed to overcome worst case challenges in EMC. Nevertheless, due to their complexity and the required number of experiments, the use of the mean contributions and safe margins are still recommended. In this context, the improvement of the estimation of the mean contributions of a physical quantity, as represented in Fig. 1 and their related maximum confidence levels become naturally important.

During EMC analysis, it is commonly accepted that only a reduced number of experiments or measurements from the so called population are accessible due to cost and computation constraints in regards of numerous random parameters. Thus, one of the important aspects, depicted in Fig. 1, is the available set of measurements (later called sample). A statistical study of the sample (stochastic process) is required so that the mean contributions can be assessed.

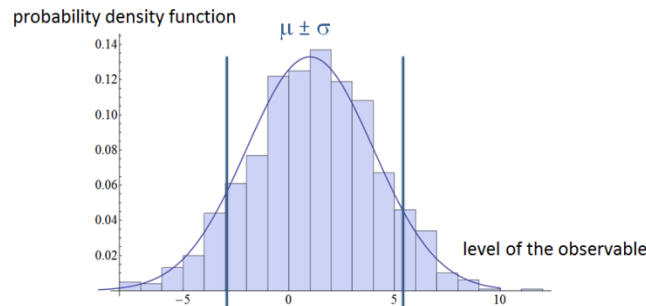


Figure 1: Probability density function of a sample S of a population P .

In 1979, Elfron came up with the bootstrapping procedure [11] allowing the estimation of the maximum confidence of a sample S in regards of a population P . A first attempt dealing with the analysis of the conducted propagation of IEMI along the power network was proposed in [12]. As it was considered as a specific test case, this paper contains supplementary details about the classical bootstrapping procedure.

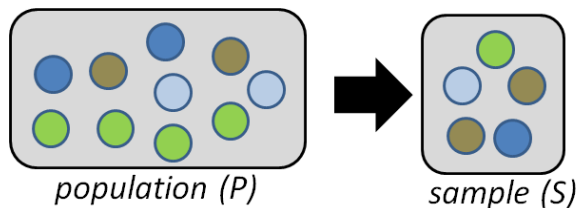


Figure 2: Schematic of the accessible set of sample S of a population P .

In this study, the need of confidence intervals estimation for EMC studies is discussed. As a key contribution, it will be shown that a potential real-time bootstrapping module involved in the processing of measurements could lead to the optimization of the required experiments.

The paper is organized as follows: in Section 2, the main lines of the three-step bootstrapping procedure are given. In Section 3, the benefit of the bootstrapping for the optimization of electromagnetic interference (EMI) and EMC tests is highlighted through two applications: an experimental radiated EMC test case and a conducted IEMI test case.

2. Bootstrapping principle

The bootstrapping procedure [11-16], introduced in 1979 by Elfron [11], is based on the derivation of *new observations* obtained by randomly taking a set of the original data (*sampling with replacement*). It can be mentioned that these methods are based on stochastic process, such as Monte Carlo, and do not require any additional information. The principle is based on a three-step procedure defined by:

1. *New observations* obtained by randomly taking a set of the original data S (*sampling with replacement*); the first step is to randomly generate with replacement new samples S_i of size m from S considering each element of S with the same probability ($1/m$) in order to estimate the reliability of the sub-set S in regards of the population P statistics while obtaining their confidence level;
2. The second step of the proposed approach refers to the definition of the statistical observable of the physical quantity; it will be defined as the mean μ and the standard deviation σ of the set S_i of independent and identically distributed (IID) values;
3. In order to perform such a task, we focus on the statistical observations convergence of the s sub-systems of the set of samples S_i . After defining the observables, such as the statistical moments of the observations, the procedure is replicated s times ($s = 1,000$ as recommended in [16]) so that the representativeness of the measured samples by the s bootstrapped sets of samples can be studied.

For preliminary experiments, the algorithm presented in Fig. 3 has been implemented. The main hypotheses are as follows: in classical EMC measurements a set of parameters are considered as random variables. The statistical moments of a physical observable are computed by selecting random configurations.

For integrating the proposed algorithm in the measurement process, we consider a fully automated measurement set-up. Each new sample is directly saved in the dataset and can be directly processed. The bootstrapping procedure is applied each time a new sample is available. Based on the confidence interval convergence and the confidence interval requirement that could be defined by an EMC tester a new sample is measured only if required. The following section will illustrate validation process based upon bootstrapping algorithm.

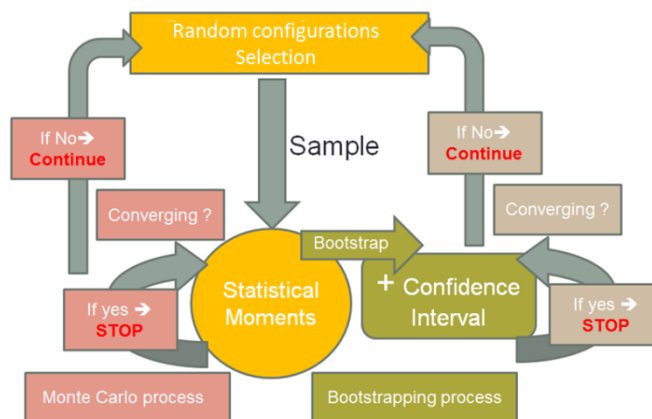


Figure 3: Schematic representation of the implemented algorithms for Monte Carlo process and Bootstrapping method comparison in real-time.

During classical EMC analysis, the number of experiments either simulated or measured is known to be a challenge due to computation and time costs. Classical approaches impose the estimation of the statistical moments convergence based on MC experiments. Nevertheless, it is argued hereafter that the measurements could be stopped as soon as a sufficient confidence level of the mean contributions or a quantile has been reached. In the next section, the benefit of the method is demonstrated through two applications related to EMC and IEMI threats.

3. Application to EMC/EMI tests

3.1 EMC radiated tests

3.1.1 Measurement set-up

This contribution relies on measurements achieved in Mode Stirred Reverberation Chamber (MSRC) from Institut Pascal embedded with a cabinet designed [17] from scratch. The goal was to manufacture a device allowing a precise control of several typical EMC parameters: slot, sizes of enclosures, location of subsystems (Fig. 4).

As depicted in Fig. 4 and schematized in Fig. 5, a metallic enclosed box (2.1 m^3) was achieved with a $0.2 \times 0.8 \text{ m}^2$ rectangular aperture at upper side. The developed moving systems allow moving an external trap (T), or an inner plate (P) jointly with a rotating unit (stirrer S) with high levels of precision ($\pm 0.02 \text{ mm}$ and $\pm 0.004^\circ$ repeatability respectively for trap / plate and stirrer).

The aim of this paper is to focus on the measurement of the mean power (P_r) received by a dipole (ETS Lindgren Model 3121C) inside the cabinet (slot entirely opened) with a spectrum analyzer ANRITSU MS2663C (9 kHz - 8.1 GHz) at frequency $f = 778.5 \text{ MHz}$.

A given power is injected in Reverberation Chamber (RC) via log-periodic antenna (ETS Lindgren Model 3144), the stirrer remaining in its initial position. Thanks to the automation of the whole process (geometrical moving and power measurements, [17]) thousands of data sets can be obtained.

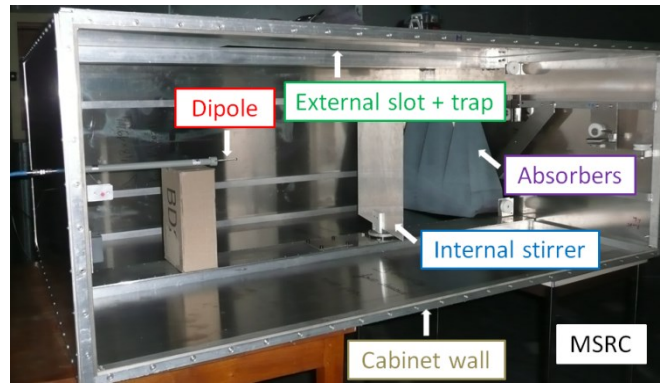


Figure 4: Inner view of the experimental cabinet including external slot, moving plate and internal stirrer [17].

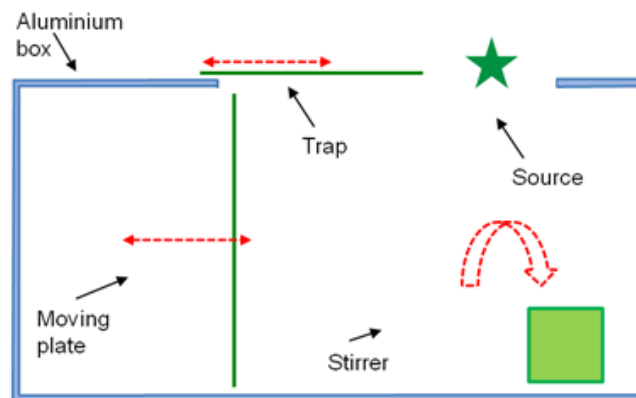


Figure 5: Schematic representation of the experimental cabinet including external slot, moving plate and internal stirrer [17].

3.1.2 Classical application

Despite all, the entire time dedicated to measurements may increase quickly due, for instance, to the standards requirements [18] for MSRC testing. In the following, thousand measurements ($m = 1,000$) will be considered, modelling a variation ± 10 mm of the moving plate (P) around its initial location. This may stand for intrinsic uncertainties of the enclosed system (cabinet) under environmental constraints (thermal, mechanical) during its normal operation.

Considering the possibility of replicating the measurement process, it could be possible to analyze the mean and standard deviation confidence intervals by analyzing the variance of the obtained mean and standard deviation as illustrated in Fig. 6. It can be observed in Fig. 6 that 1,000 measurements allow for a good estimation of the statistical moments (the variation is less than 1 % around the estimated mean contributions).

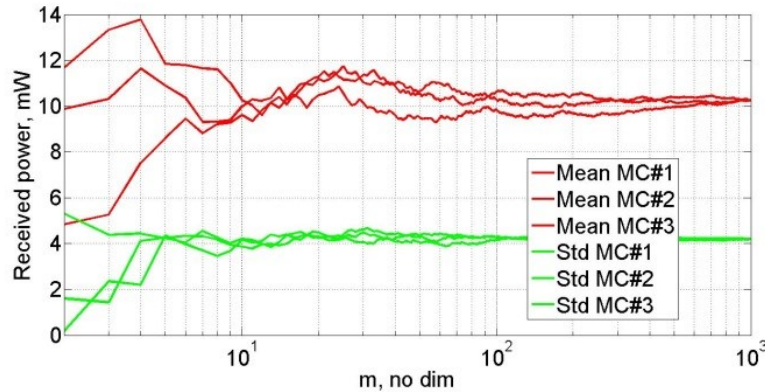


Figure 6: Mean and standard deviation of three set of random selections of measurement in regards of the length (m) of the samples.

Nevertheless, in classical EMC testing due to the time constraints, it is clearly inappropriate to perform more than once a single test. Thus, the mean contributions are obtained from one sample only. Table 1 gives an overview of the mean contributions obtained from crude Monte Carlo (MC) computations to one sample as it is classically applied.

Table 1: MC results

| Statistics | Received Power (MC) in mW |
|------------|---------------------------|
| Mean | 10.251 |
| Std | 4.192 |

Once the environment has been characterized, the analysis could lead to the hardening of a potential electronic device susceptible to parasitic field. Nevertheless, the lack of information about the mean confidence interval could lead to the underestimation of the risk. As a result the bootstrapping procedure presented in Section 2 is applied to the set of samples.

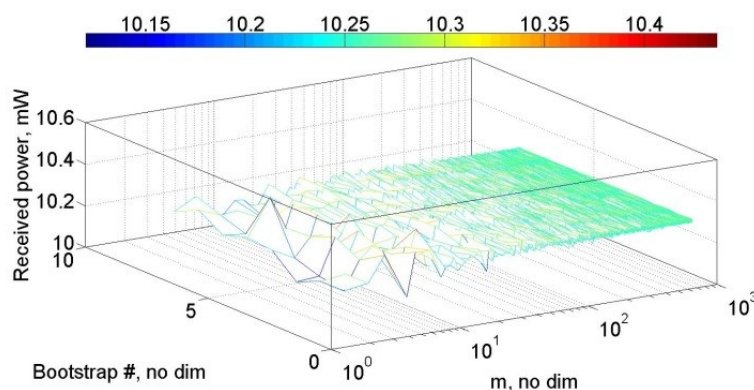


Figure 7: Random selection (8 for graph readability) of samples applying the bootstrap to the received power mean in regards of the length (m) of the selected samples

A first representation is proposed in Fig. 7 in which it can be observed the evolution of the received mean power for a set of random selection by bootstrap in regards of the length (m) of samples. It can be mentioned that the estimated means are quickly converging to a value around

10.258 mW. Similarly, Fig. 7 provides an overview of eight different assessments of standard deviation using the bootstrap. It can be also noticed that convergence rate is quick towards 4.189 mW.

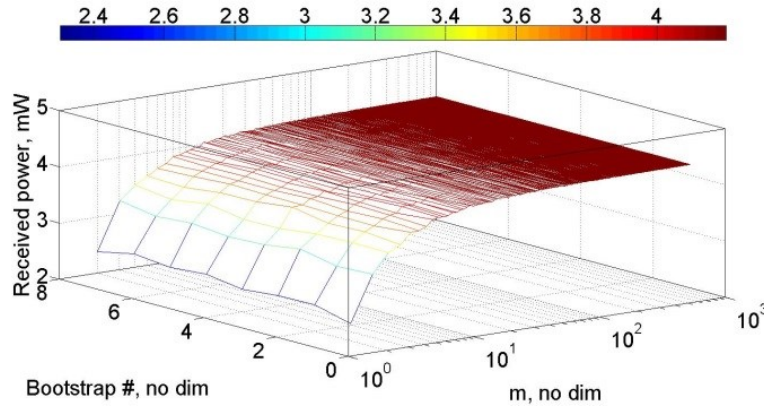


Figure 8: Random selection (8 for graph readability) of samples applying the bootstrap to the received power standard deviation in regards of the length (m) of the selected samples.

Using the random selections of samples by the proposed approach it is now possible to compute the confidence interval. Table 2 is obtained by applying the three-step procedure (section 2) to the measurements.

Table 2: Results for Bootstrap ($M=1,000$) in mW

| Statistics | Received Power (Bootstrap) in mW | |
|---------------|----------------------------------|------------------------|
| | mean ($s = 1,000$) | std ($s = 1,000$) |
| mean | 10.258 | 4.189 |
| Quantile 0.05 | 10.052 | 4.091 |
| Quantile 0.95 | 10.474 | 4.289 |

The coefficient of variation (rate between standard deviation and mean) derived from Table 2 validates the good convergence of the results both for the mean and standard deviation of the received power (respectively around 1.2 % and 1.4 %). The computed mean contributions by MC are 10.251 mW and 4.192 mW respectively. The last statistical moments computed with the bootstrap methods (i.e. mean, Fig. 7, and standard deviation, Fig. 8) are 10.258 mW with a confidence interval in [10.052; 10.474] mW and 4.189 mW with a related confidence interval in [4.091; 4.289] mW. It shows a good agreement between bootstrapped mean and standard deviation obtained with $m = 1,000$ comparatively to the corresponding statistical moments obtained with MC. Moreover, useful information about the confidence intervals, given by applying the bootstrap, is summarized in Table 2. The 0.05 and 0.95 quantiles' assessment of the bootstrapped mean and standard deviation which show the confidence levels given from bootstrapped data.

Finally, the bootstrapping procedure enables to enhance the statistical study of the mean contributions as it interestingly provides the related confidence interval. In the next Section, we

seek to involve the confidence interval as an alternative stop condition to the classical MC method.

3.1.3 Application and validation on mean contributions

In order to estimate the pertinence of the proposed approach, the convergence of the bootstrapping means and standard deviations are analyzed for each new value added to the original set of measurements. Thus, the length of the bootstrapped samples is taken in $[2; 3; \dots; m = 1,000]$ where m denotes the length of the dataset (the number of samples involved in the re-sampling process). Defining a constraint confidence level, the need of an additional experiment is iteratively and in real-time estimated.

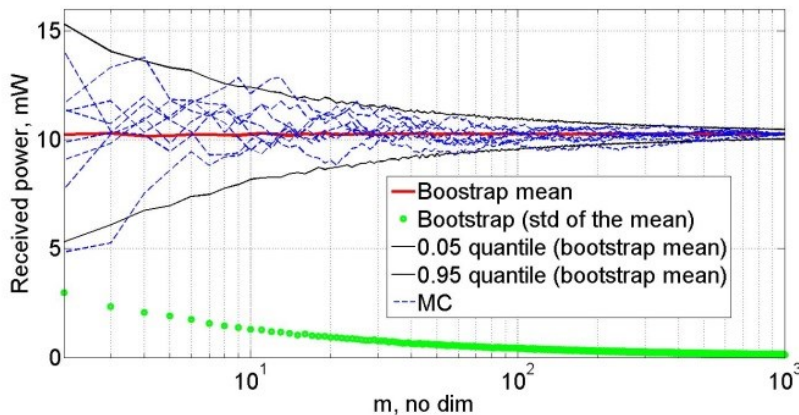


Figure 9: Mean (red), standard deviation (green) and confidence interval (black) for the bootstrapped means and 8 random Monte Carlo selections (blue) for illustration purpose in regards of the length (m) of the selected samples.

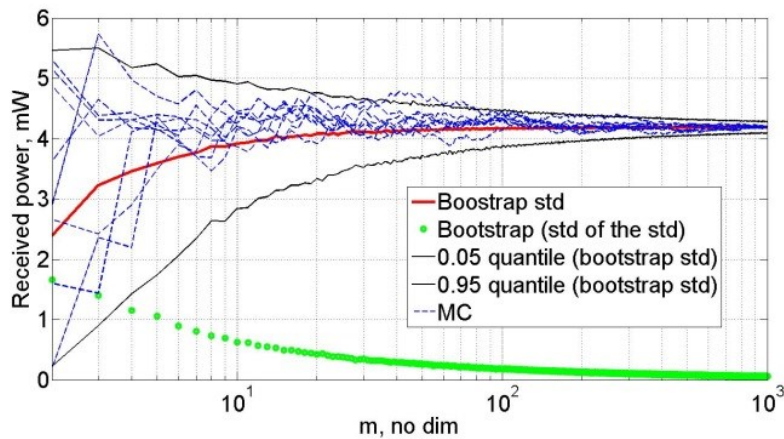


Figure 10: Mean (red), standard deviation (green) and confidence interval (black) for the bootstrapped standard deviations and 8 random Monte Carlo selections (blue) for illustration purpose in regards of the length (m) of the selected samples.

Figs. 9 and 10 provide an overview of this potential iterative and real-time assessment applied to the mean and standard deviation. In supplement, a set of random Monte Carlo simulations has

been selected for illustrative purpose. Indeed, the mean behavior computed from bootstrap is provided in Fig. 9.

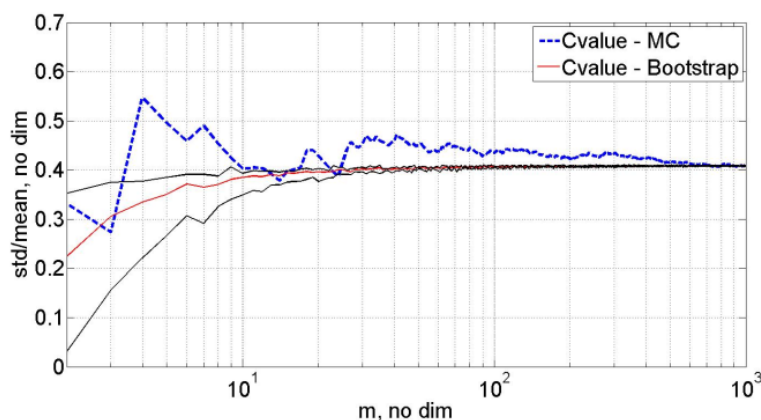


Figure 11: Standard deviation to mean ratios for MC (blue), bootstrap (red) and related standard deviation confidence interval to mean confidence interval ratios obtained by 1,000 bootstrap replications (black) in regards of the size m of the selected samples.

First, it is shown a quick convergence since $m = 3$ gives an accurate assessment of the mean received power for the whole set of bootstrap achievements (8 different bootstrap realizations, only one shown in Fig. 9).

The standard deviation to the mean ratios in regards of the size of the samples (m) with their related confidence interval ratios are shown in Fig. 11. It points out the quick bootstrap convergence comparatively to MC. As expected, the confidence intervals given through quantiles' assessment (from 0.05th and 0.95th quantiles) provide a close view of the bootstrap spread.

Comparatively to MC convergence, the 0.05 and 0.95 quantiles from bootstrapped standard-deviations offer a realistic view of the data set dispersion. It can be observed that the bootstrapping results contain both the Monte Carlo outcomes (mean contributions convergence) and the related confidence interval of the samples.

Given particular assumptions about the authorized margins (standards [18-19] for instance), bootstrapping allows a precise optimization of the number of measured samples required with high confidence levels. Computation of standard deviation in Fig. 10 validates the quick convergence relatively to parameter m ($m = 20$). Moreover, it can be noticed that results from bootstrapping procedure provide interesting confidence intervals in comparison with MC (Figs. 9-12).

3.1.4 Application and validation on high quantiles

One can seek the confidence interval of a very high quantile. The proposed algorithm has been applied to values having a low probability. Fig. 12 deals with quantile at 95 % obtained by bootstrap. As it can be observed, the convergence of MC results is quite slow comparatively to treatments based upon bootstrapping procedures.

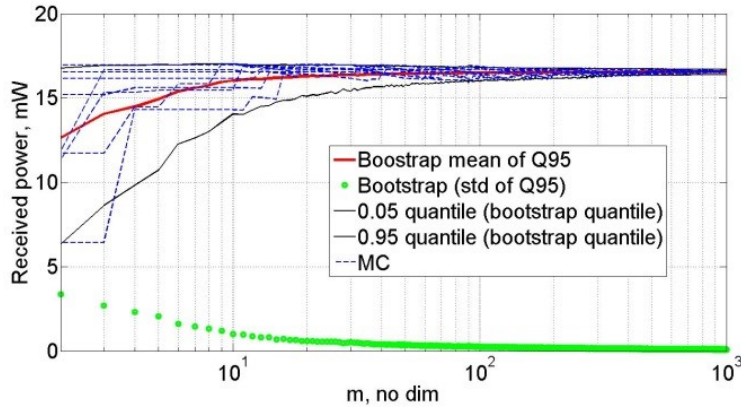


Figure 12: Mean (red), standard deviation (green) and maximum confidence interval (black) for the bootstrapped 95th- quantile (Q95) and 8 random Monte Carlo selections (blue) for illustration purpose in regards of the length (m) of the selected samples.

Since quantiles are intrinsically linked with tail behavior of statistical distribution laws, a precise assessment of confident levels is again of fundamental interest. Fig. 12 shows the good agreement between confidence intervals from Bootstrapping and MC results. Indeed, bootstrap predictions (8 different realizations) efficiently provide in real-time safety margins for computing mean of quantile at 95% of received power. Assuming a given 1mW-threshold for received power confidence intervals, bootstrap method fully complies with previous requirements with $m = 20$, even considering various bootstrap achievements (e.g. eight in Fig. 12). The state is far more difficult in regards of MC cases since results remain widely spread relying on crude MC quantiles' assessment in Fig. 12. In this framework, the 0.05 and 0.95 quantiles of the m bootstrapped 0.95-*th* quantiles (quantile at 95 %) gives a quick but precise estimation how results may be compliant with given recommendations (standards for instance).

3.1.5 Bootstrap procedure and Central Limit Theorem

The *Central Limit Theorem* [20] (CLT) defines the conditions in which the distribution of the normalized set of samples mean and standard deviation (samples are considered as independent variables – the set-up [17] depicted in Fig. 3 has been mechanically designed so that measurements are clearly uncorrelated) $S = \{S_1, S_2, \dots, S_n\}$, assuming that each sample S_i have a well-defined expectation value and a well-defined variance, converges toward the Normal distribution when n is increasing ($n \rightarrow \text{inf}$) regardless of their underlying distribution. The distribution is assumed to converge to a Normal distribution with mean and standard deviation parameters defined by $n \cdot \varphi$ and $\sigma \cdot \sqrt{n}$.

In case of the adjusted distributions for EMC observable modelling, the Normal distribution is not well suitable but is *often* used. Interestingly, it is admitted that for a sample randomly taken from a Normal distribution of length m from M (*length of the complete dataset*), the computed mean of each sample is known to be related to one over the squared root of the length of the dataset.

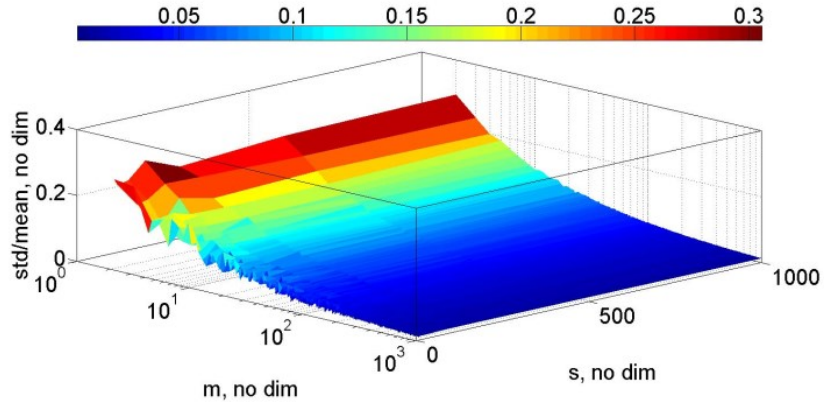


Figure 13: Standard deviation to mean ratios in regards of the length (m) of the selected samples and the number (s) of the bootstrap replications.

As a result, the standard deviation to the mean ratio of a sample composed of the mean and standard deviation of each generated sample is converging toward the value of $C_{\text{value}} = 1/\sqrt{n}$ (for $n \rightarrow \text{inf}$, $C_{\text{value}} \rightarrow 0$).

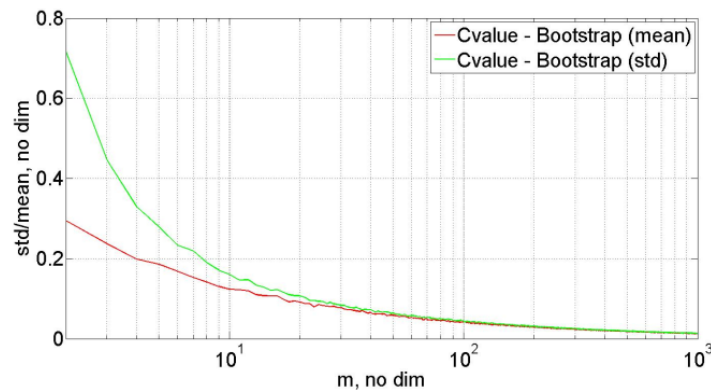


Figure 14: Standard deviation to mean ratios of the 1,000 bootstrapped means (red) and of the 1,000 bootstrapped standard deviations (green) in regards of the length (m) of the selected samples.

The need for new samples requires the replication of a large number of experiments. Nevertheless, thanks to the bootstrapping procedure random sample S_i can be simulated while adding new measurements. The accuracy of the convergence (hypothesis given by the CLT) toward the C_{value} , when investigate in the framework of the bootstrapping procedure, is directly related to the number and the length of the bootstrapped samples. Note that in our case, the length of the sample is evolving in regards of the parameters s and m .

In order to have a clue on the importance of the size s of sample, the C_{value} has been computed for sample size s in [10; 20; 50; 100; 200; 500; 1,000]. Fig. 13 gives an overview of the standard deviation to mean ratios (here called C_{values}) in regards of the bootstrapping iteration number s and the size of the sample m , derived from mean and standard deviation assessments of inner antenna received power (Fig. 3).

Again, it may be pointed out that for a reduced number of measurements ($m = 20$), the convergence of the standard deviation to mean ratio of the bootstrapped samples (C_{values} converging toward a value of 0.10) allows the assessment and validation of the CLT convergence hypothesis.

As for highlight purpose, the specific case of $s = 1,000$ and $m = 1,000$ is depicted in Fig. 14. The governing trend of both curves (red and green ones respectively in Fig. 14) validates the Central Limit Hypothesis (CLH) of the standard to mean ratio convergence.

3.2 Conducted propagation of IEMI along the power network

Several studies [1, 2] demonstrated that electronic devices connected to the low voltage power networks are sensitive to intentional electromagnetic interferences (IEMI) [3-6]. In order to reduce the threat of IEMI to tolerable levels, adequate protective devices can be inserted along the power grid. Thus, the estimation of induced voltages at the equipment level is important. We propose in this section to demonstrate the benefit of the bootstrapping procedure in the estimation of mean contributions of the risks and their related confidence interval.

3.2.1 Measurement set-up

We first propose a summary of the measurement campaign of the IEMI conducted propagation along the power network performed in February 2013 in the EMC Laboratory of the EPFL Switzerland by Nicolas Mora (researcher at the EPFL) and Chaouki Kasmi (researcher at ANSSI) under the supervision of Prof. Farhad Rachidi.

A full custom experimental setup has been designed by the EMC laboratory of the Swiss Federal Institute of Technology in Lausanne in order to analyse the conducted propagation of electromagnetic waves along the low voltage power networks as they are typically installed in Switzerland [21, 22]. Each power socket is connected with a Terra-Terra cable from the brand NEXANS.

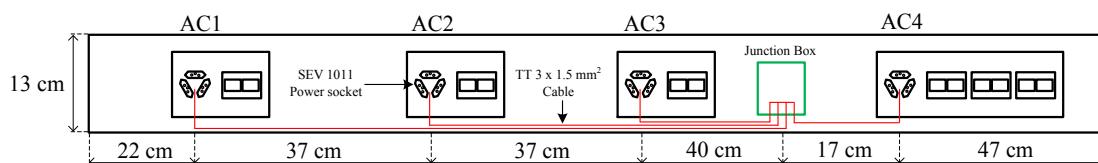


Figure 15: Electrical raceway under study [22, 23].

The NEXANS cable is composed of three coated wires having a cross-section of 1.5 mm^2 that are used for the connection of the Phase, Neutral and Protective Earth lines of the distribution network, and are tested to withstand a maximum voltage of 1 kV before the dielectric breakdown. The power cables are connected in a star configuration starting at each of the power sockets (AC1, AC2, AC3 and AC4) and ending at a junction box. The setup was worth to measure the transfer functions between different power sockets with different techniques in the frequency domain and the time domain.

3.2.2 Conducted propagation of electromagnetic interferences

Many studies, summarized in [21, 22], have shown that the type and the number of connected appliances induce significant variation of the propagation path. In order to reproduce a scenario that is close to the ones expected in real situations, transfer function measurements have been

performed while different appliances were randomly connected. The tests were carried out by injecting a signal to one end of the power network (AC1), between phase and neutral conductors (neutral and protective earth conductors are short-circuited) with a signal generator, and simultaneously measuring the amplitude of the signal at the other end with a spectrum analyzer, as depicted in Fig. 16.

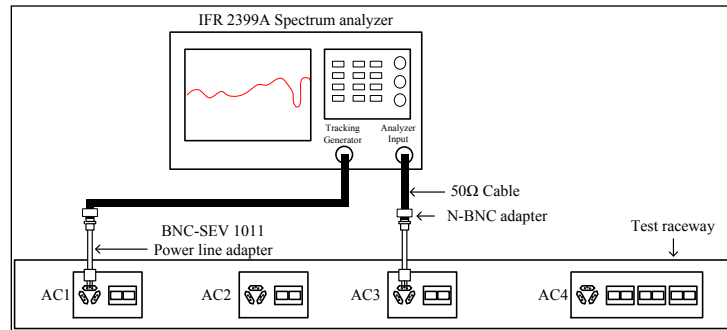


Figure 16: Experimental process in the semi-anechoic chamber at the EMC Laboratory of EPFL [21, 22].

The power transfer function has been obtained from 150 kHz – 200 MHz. Note that in these experiments, it has been considered that the transfer function is computed as the ratio between the power measured at the analyzer input and the emitted power at the tracking generator output. This means that the 50 Ω to power network adapters have been considered as low voltage power network extensions.

3.2.3 Effects induced by connected electronic devices

The experimental setup schematized in Fig. 16 was used for measuring the output power at the socket levels in a loaded status. In the loaded status tests, random electrical appliances were connected to the raceway sockets for each measurement.



Figure 17: Experimental process in the semi-anechoic chamber at the EMC Laboratory of EPFL [21, 22].

In order to statistically investigate the effects induced by the type and number of connected appliances, we measured about 200 transfer functions between two power sockets (the number of measurements between the sockets AC1-AC2, AC1-AC3 and AC1-AC4 are 200, 200 and 196 respectively) by simultaneously and randomly connecting seven electronic devices (e.g. lights, computers, computer screen...) as shown in Fig. 17. In our experiments, it has been noticed an

important decrease of the propagated energy at low frequencies once the raceway is loaded as shown in Fig. 18.

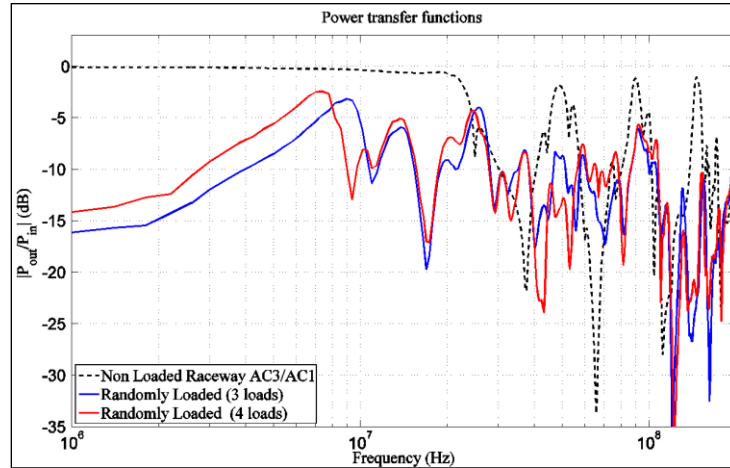


Figure 18: Power transfer function magnitude between the two power sockets AC1-AC3 with the network unloaded and randomly loaded [21, 22]

It can be pointed out that transmitted power between the sockets is highly sensitive to the number and type of connected electronic devices. We propose not to apply the bootstrapping procedure using the random power transfer functions [21, 22] to derive the maximum confidence intervals of the mean contributions of the expected voltage at the power sockets level (AC2, AC3 and AC4) resulting from an injection of a 1 V generator, which remains connected to socket AC1.

3.2.4 Analysis of the mean contributions and high quantiles of the induced voltages

The mean contributions of the induced voltage in case of 200 random configurations and 196 random configurations for AC2, AC3 and AC4 respectively assessed from the straightforward statistical analysis are proposed in Tables 3, 4 and 5. For each socket, the MC analysis is proposed for comparison purpose with the bootstrapping procedure results. Results are provided for socket AC2 here after. Concerning the sockets AC3 and AC4, results are provided in the annexes A1. As depending on the impedances of connected loads, high and low attenuation can be observed in Fig. 18, we considered two frequencies for applying the so called bootstrapping procedure.

Socket AC2

Table 3: MC results of the induced voltage on AC2

| position | Frequency (MHz) | Mean (mV) | Standard deviation (mV) | Quantile 5% (mV) | Quantile 95% (mV) |
|----------|-----------------|-----------|-------------------------|------------------|-------------------|
| AC2 | 4.58 | 185.28 | 71.08 | 90.56 | 317.40 |
| | 160.1 | 100.16 | 28.75 | 44.46 | 134.27 |

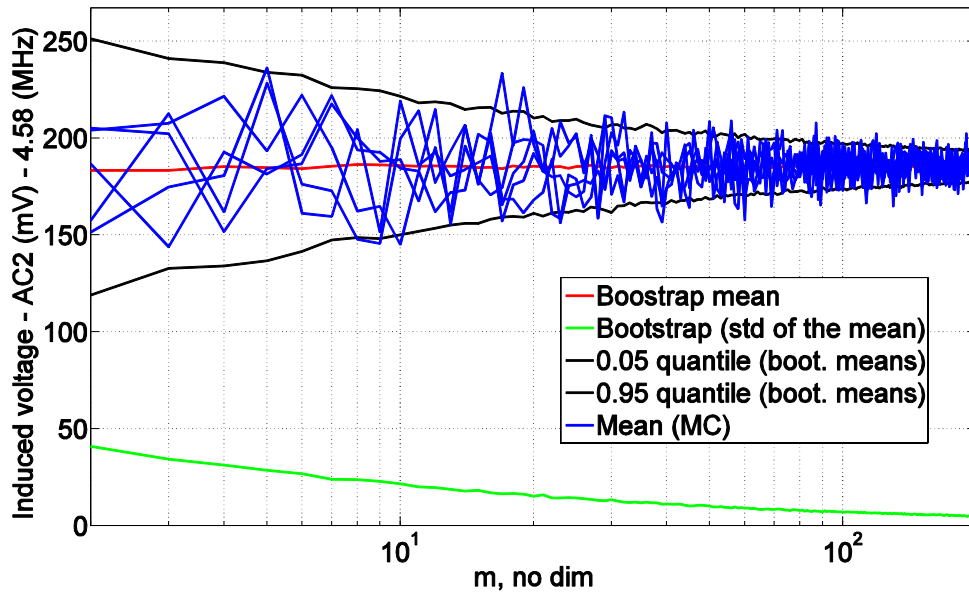


Figure 19: Mean (red), standard deviation (green) and confidence interval (black) for the bootstrapped means and 5 random Monte Carlo selections (blue) for illustration purpose in regards of the length (m) of the selected samples at 4.58 MHz.

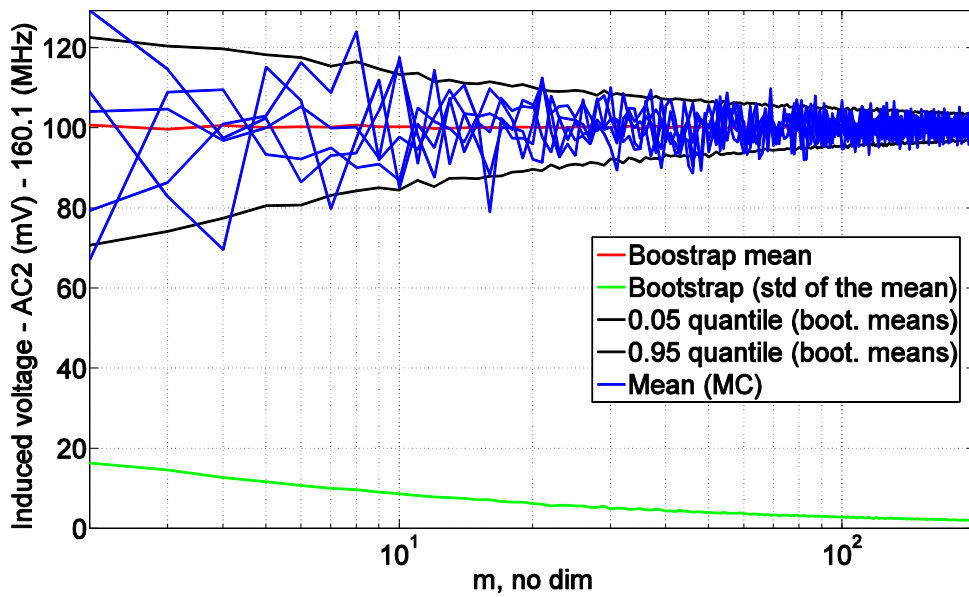


Figure 20: Mean (red), standard deviation (green) and confidence interval (black) for the bootstrapped means and 5 random Monte Carlo selections (blue) for illustration purpose in regards of the length (m) of the selected samples at 160.1 MHz.

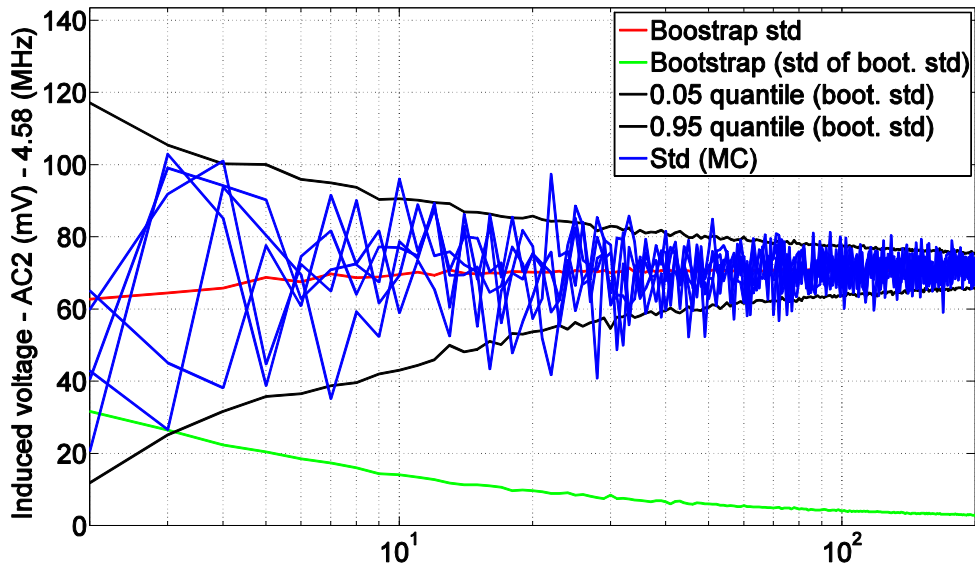


Figure 21: Mean (red), standard deviation (green) and confidence interval (black) for the bootstrapped standard deviations and 5 random Monte Carlo selections (blue) for illustration purpose in regards of the length (m) of the selected samples at 4.58 MHz.

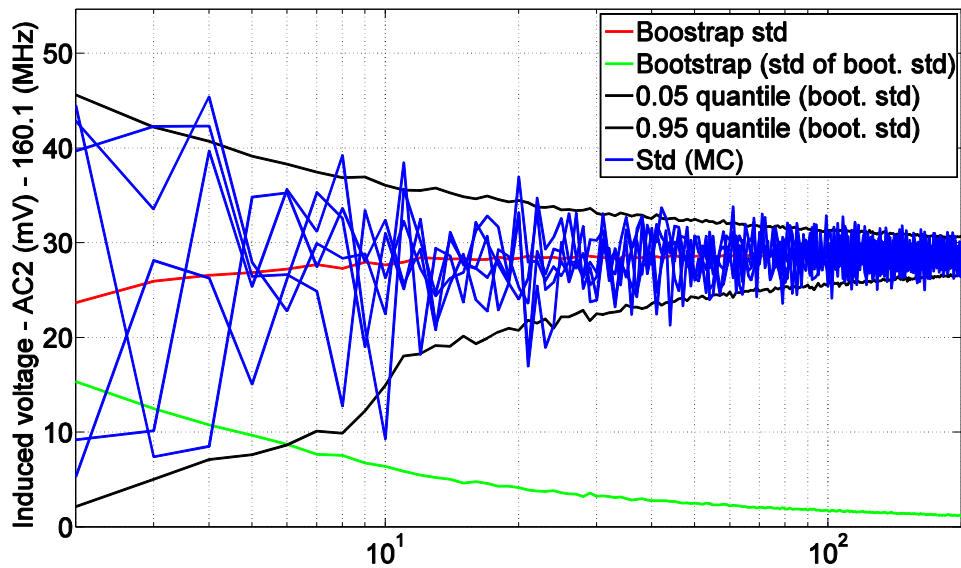


Figure 22: Mean (red), standard deviation (green) and confidence interval (black) for the bootstrapped standard deviations and 5 random Monte Carlo selections (blue) for illustration purpose in regards of the length (m) of the selected samples at 160.1 MHz.

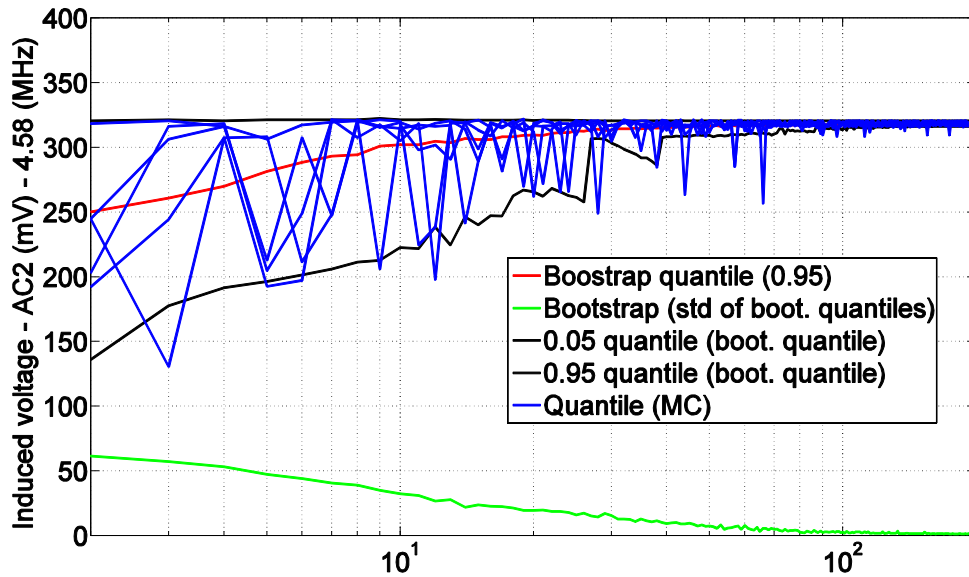


Figure 23: Mean (red), standard deviation (green) and maximum confidence interval (black) for the bootstrapped 95th- quantile (Q95) and 5 random Monte Carlo selections (blue) for illustration purpose in regards of the length (m) of the selected samples at 4.58 MHz.

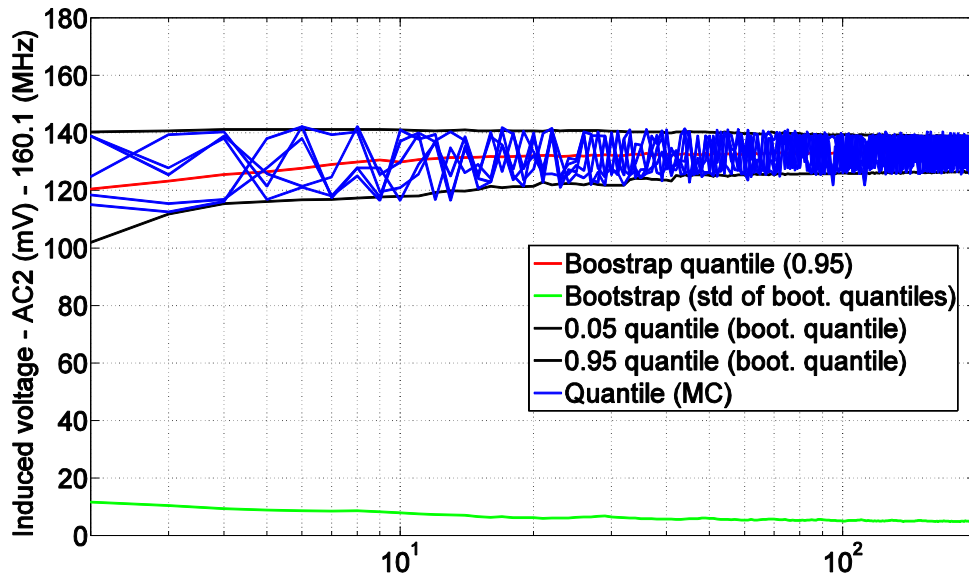


Figure 24: Mean (red), standard deviation (green) and maximum confidence interval (black) for the bootstrapped 95th- quantile (Q95) and 5 random Monte Carlo selections (blue) for illustration purpose in regards of the length (m) of the selected samples 160.1 MHz.

Figs. 19, 21 and 23 provide an overview of an iterative bootstrapping assessment applied to the mean, standard deviation and 0.95 quantile at 4.58 MHz. Figs. 20, 22 and 24 provide an overview of an iterative bootstrapping assessment applied to the mean, standard deviation and 0.95 quantile

at 160.1 MHz. In supplement, a set of 5 random Monte Carlo simulations has been selected for illustrative purpose.

Indeed, the mean behavior computed from bootstrap is provided as depicted in Figs. 19-22. Again, it can be observed that results provided by the bootstrapping procedure allows for estimating the mean contribution and their related confidence intervals. Moreover, a quick estimation of statistical moments can be performed thanks to the proposed algorithm. Finally, it can be pointed out Figs. 23 and 24 that high quantiles can be efficiently assessed thanks to the confidence intervals.

Socket AC3 (Figures 25-30 and Table 4, Annex A)

Figs. 25 and 26, 27 and 28, 29 and 30 provide an overview of an iterative bootstrapping assessment applied respectively to the mean, standard deviation and 0.95 quantile. In supplement, a set of 5 random Monte Carlo simulations has been selected for illustrative purpose. Indeed, the statistical behavior computed from bootstrap is provided are depicted regarding socket AC3.

Socket AC4 (Figures 31-36 and Table 5, Annex A)

Similarly to Figs. 25-30, Figs. 31-36 offer a quick view of the mean (Figs. 31-32), standard deviation (Figs. 33-34) and 0.95-quantile (Figs. 35-36) obtained from bootstrapping procedure.

Providing trustworthy confident intervals is all the more important than the dispersion of results may lead to major uncertainties (especially regarding quantiles obtained from MC, Fig. 36). By efficiently allowing iterative assessment, bootstrap ensures real-time reliable decisions about measurement.

4. Conclusion

This contribution addressed the use of bootstrap process for EMC/EMI tests optimization. The use of a dedicated and embedded system jointly with a bootstrap module highlighted the benefit offered by this technique: precise confidence intervals were provided with a limited number of experiments (e.g. decreasing the experimental time and costs). Moreover, the Central Limit Hypothesis (CLH) has been tested considering the bootstrapping procedure for generating samples from the selected and tested random configuration when adding a new measurement to the dataset. We applied the proposed method to two applications related to EMC and IEMI studies:

Application 1: The device designed in this work is representative of a large diversity of EMC protections: the process may be useful for standard [18] assessment of the shielding effectiveness of real systems. Future work will demonstrate the interest of bootstrap for realistic radiated EMC testing [19];

Application 2: The propagation of electromagnetic interference along the power network has been evaluated in the framework of the test set-up summarized in this paper. Thanks to the analysis of the induced voltage at equipment level and the reliable analysis of the statistical moments and high quantiles combined with their confidence intervals, it is possible to define adequate protective devices for hardening the power network.

The MC convergence has been optimized based on the mean and standard deviation. The statistical moments above (e.g. skewness, kurtosis) convergence could also be checked so that the characteristic function related to the empirical distribution of the MC sample could be assessed. This could lead to a further analysis made with higher size of sample. The application of the bootstrapping procedure could bring additional information about the shape of the distribution and its tails while checking that the shape of the bootstrapping samples have equivalent values (potential bias added by the bootstrapping process on higher statistical moments). In this framework, we will consider more complex cases increasing the complexity of EMC realistic radiated tests (e.g. following requirements from [19]). The validity of CLT may be crucial in regards of the optimization of such testing procedures. Further work will be dedicated to these issues.

References

- [1] D. Nitsch, M. Camp, F. Sabath, et al., "Susceptibility of some electronic equipment to HPEM threats", *Electromagnetic Compatibility, IEEE Transactions on*, vol. 46, pp. 380-389, 2004.
- [2] F. Brauer, F. Sabath, and J.L. Haseborg, "Susceptibility of IT network systems to interferences by HPEM", *Electromagnetic Compatibility, IEEE International Symposium on*, pp. 237-242, 2009.
- [3] N. Mora, C. Kasmi, F. Rachidi, M. Hélier, and M. Darces, "Modeling and measurement of the propagation along low voltage power networks for IEMI studies", *Technical report*, February, 2013.
- [4] C. Kasmi, "Application de la topologie électromagnétique à la modélisation du réseau énergétique basse tension : étude statistique des perturbations conduites", *PhD thesis*, UPMC, December, 2013.
- [5] Y. V. Parfenov, L. N. Zdoukhov, W. A. Radasky, and M. Ianoz, "Conducted IEMI threats for commercial buildings", *Electromagnetic Compatibility, IEEE Transactions on*, vol. 46, pp.404-411, 2004.
- [6] D. Mansson, R. Thottappillil, and M. Backstrom, "Propagation of UWB Transients in Low-Voltage Power Installation Networks", *Electromagnetic Compatibility, IEEE Transactions on*, vol. 50, pp.619-629, 2008.
- [7] G. Gradoni and L.R. Arnaut, "Generalized Extreme-Value Distributions of Power Near a Boundary Inside Electromagnetic Reverberation Chambers", *Electromagnetic Compatibility, IEEE Transactions on*, vol.52, no.3, pp.506,515, Aug. 2010.
- [8] C. Kasmi, M. Hélier, M. Darces, and E. Prouff, "Generalised Pareto distribution for extreme value modelling in Electromagnetic Compatibility", *Electronics Letters* 49, Vol. 5, pp. 334-335, 2013.
- [9] M. Larbi, P. Besnier, B. Pecqueux, "Probability of EMC Failure and Sensitivity Analysis With Regard to Uncertain Variables by Reliability Methods", *Electromagnetic Compatibility, IEEE Transactions on*, vol. 57, no. 2, April 2015.
- [10] A. Kouassi, J-M. Bourinet, S. Lalléchère, P. Bonnet, and M. Fogli, "Safety assessment of a transmission line with EMC requirements", XXXIth URSI GASS, Beijing, China, August 2014.
- [11] B. Efron and R. J. Tibshirani, "An introduction to the bootstrap", Chapman and Hall, London, 1993.
- [12] C. Kasmi, M. Hélier, M. Darces, and E. Prouff, "Application of a bootstrapping procedure to the analysis of the conducted propagation of electromagnetic interferences along the power network", *Kleineheubach Tagung*, Miltenberg, Germany, September 2014.
- [13] G. J. Babu and K. Singh, "Inference on means using the bootstrap", *Ann. Stat.* Vol. 11, pp.9 99-1003, New-York, 1983.
- [14] Y. Zhang, D. Hatzinakos, and A.N. Venetsanopoulos, "Bootstrapping techniques in the estimation of higher-order cumulants from short data records", *Acoustics, Speech, and Signal Processing - ICASSP-93, IEEE International Conference on*, vol.4, no., pp.200,203 vol.4, 27-30 April 1993.
- [15] A. Cucchiarelli and P. Velardi, "A statistical technique for bootstrapping available resources for proper nouns classification", *Information Intelligence and Systems*, 1999. *Proceedings of International Conference on*, vol., no., pp.429-435, 1999.
- [16] F. Harrell, "Regression Modeling Strategies: With applications to linear models, logistic regression, and survival analysis", Springer, 2001.
- [17] S. Lalléchère, S. Girard, P. Bonnet, and F. Paladian, "Stochastic approaches for ElectroMagnetic Compatibility: a paradigm from complex reverberating enclosures", in *Proc. ESA Workshop on EMC*, Venice, Italy, May 2012.
- [18] International Electrotechnical Commission (IEC), IEC 61000-4-21, EMC - Part 4-21: Testing and measurement techniques - Reverberation chamber test methods, 2003.
- [19] IEEE standard method for measuring the shielding effectiveness of enclosures and boxes having all dimensions between 0.1 m and 2 m, 2013.
- [20] J. Rice, *Mathematical Statistics and Data Analysis*, Second ed., Duxbury Press, ISBN 0-534-20934-3, 1995.
- [21] N. Mora, C. Kasmi, F. Rachidi, M. Hélier, M. Darces, "Modeling and measurement of the propagation along low voltage power networks for IEMI studies", *Technical report*, February, 2013.
- [22] C. Kasmi, "Application de la topologie électromagnétique à la modélisation du réseau énergétique basse tension : étude statistique des perturbations conduites", *PhD thesis* (written in English), December, 2013.

ANNEX A

Socket AC3

Table 4: MC results of the induced voltage on AC3

| position | Frequency (MHz) | Mean (mV) | Standard deviation (mV) | Quantile 5% (mV) | Quantile 95% (mV) |
|----------|-----------------|-----------|-------------------------|------------------|-------------------|
| AC3 | 4.58 | 185.28 | 71.08 | 90.56 | 317.41 |
| | 160.1 | 54.92 | 43.65 | 15.06 | 140.57 |

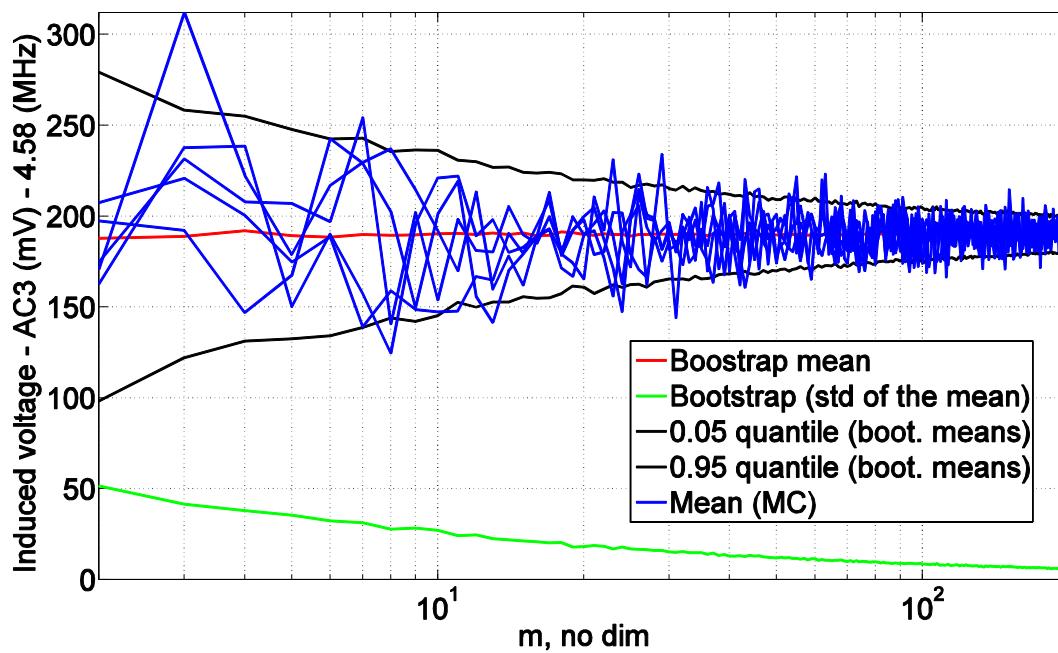


Figure 25: Mean (red), standard deviation (green) and confidence interval (black) for the bootstrapped means and 5 random Monte Carlo selections (blue) for illustration purpose in regards of the length (m) of the selected samples at 4.58 MHz.

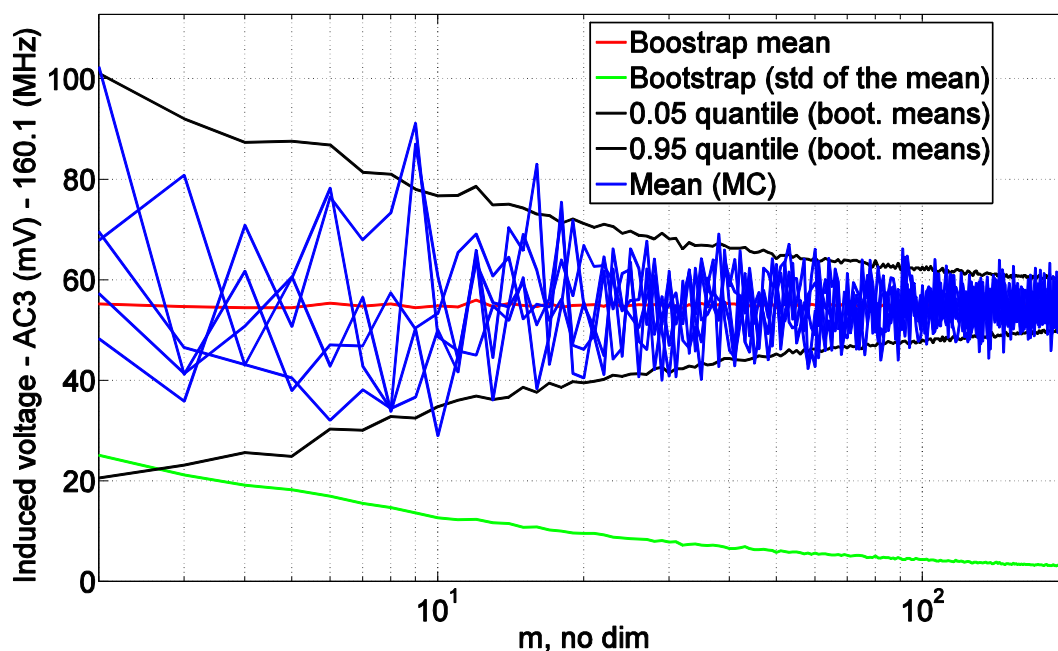


Figure 26: Mean (red), standard deviation (green) and confidence interval (black) for the bootstrapped means and 5 random Monte Carlo selections (blue) for illustration purpose in regards of the length (m) of the selected samples at 160.1 MHz.

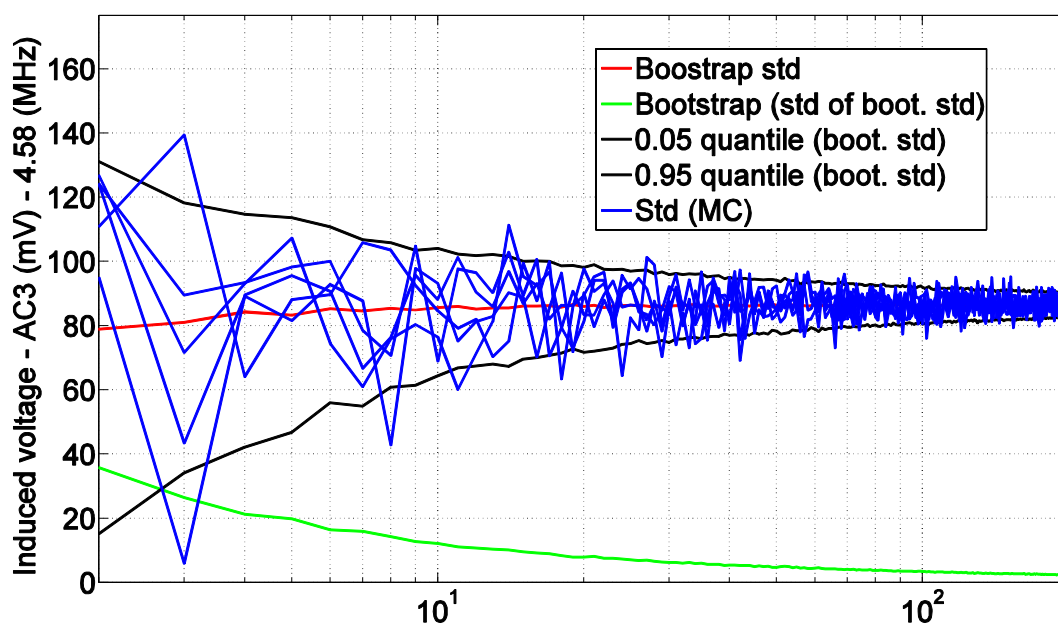


Figure 27: Mean (red), standard deviation (green) and confidence interval (black) for the bootstrapped standard deviations and 5 random Monte Carlo selections (blue) for illustration purpose in regards of the length (m) of the selected samples at 4.58 MHz.

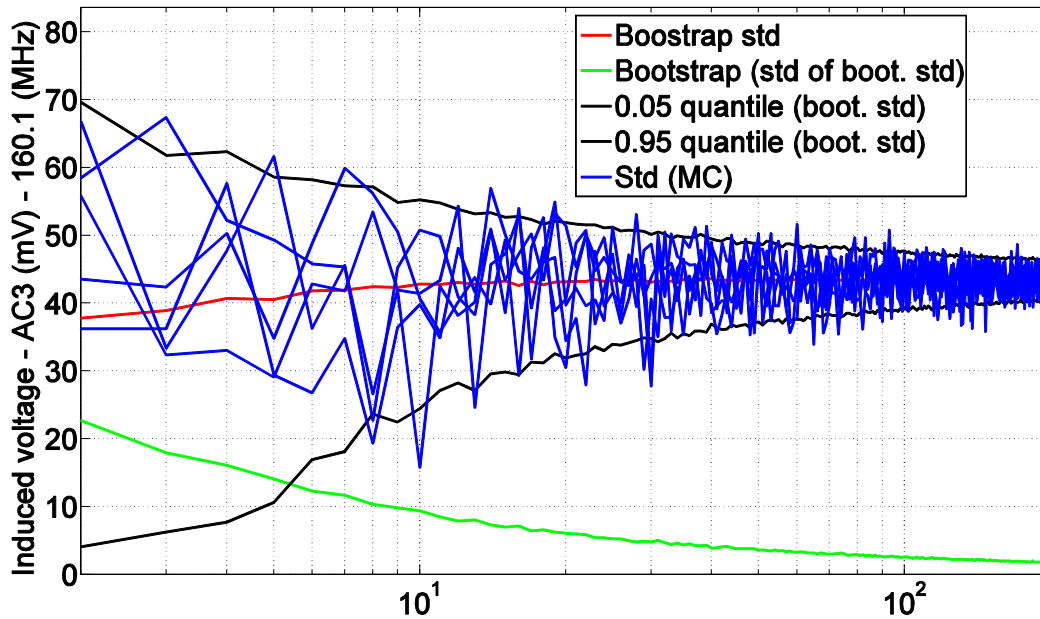


Figure 28: Mean (red), standard deviation (green) and confidence interval (black) for the bootstrapped standard deviations and 5 random Monte Carlo selections (blue) for illustration purpose in regards of the length (m) of the selected samples at 160.1 MHz.

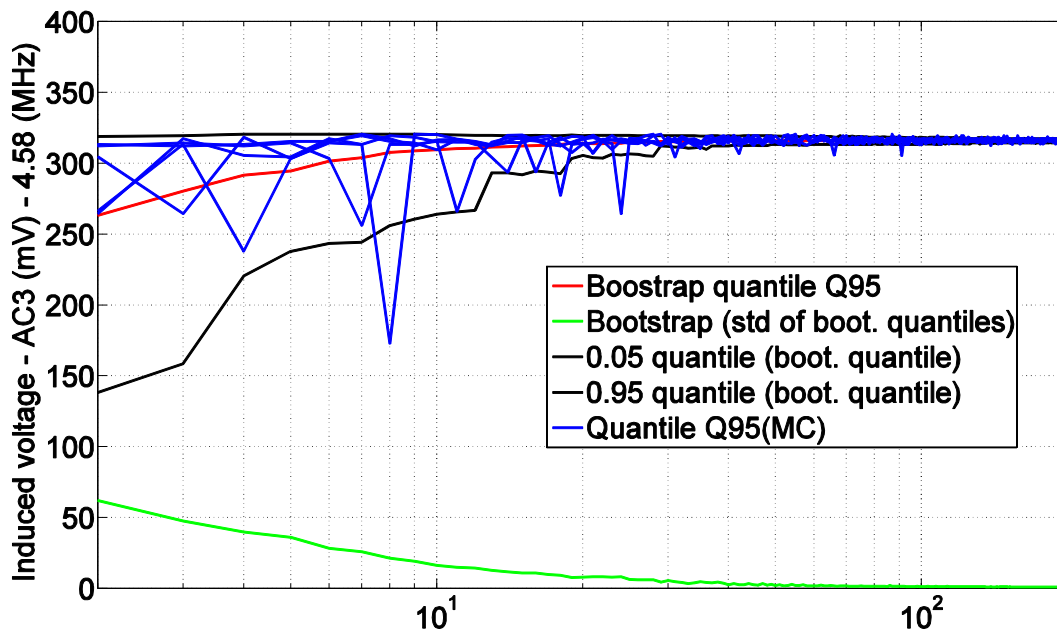


Figure 29: Mean (red), standard deviation (green) and maximum confidence interval (black) for the bootstrapped 95th- quantile (Q95) and 5 random Monte Carlo selections (blue) for illustration purpose in regards of the length (m) of the selected samples at 4.58 MHz.

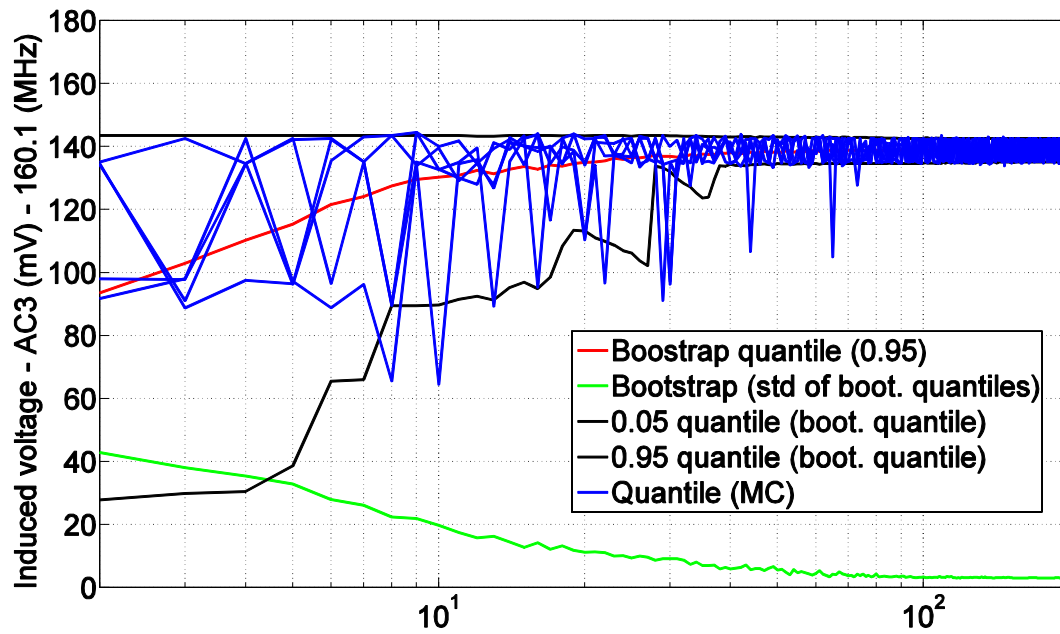


Figure 30: Mean (red), standard deviation (green) and maximum confidence interval (black) for the bootstrapped 95th- quantile (Q95) and 5 random Monte Carlo selections (blue) for illustration purpose in regards of the length (m) of the selected samples at 160.1 MHz.

Socket AC4**Table 5: MC results of the induced voltage on AC3**

| position | Frequency (MHz) | Mean (mV) | Standard deviation (mV) | Quantile 5% (mV) | Quantile 95% (mV) |
|----------|-----------------|-----------|-------------------------|------------------|-------------------|
| AC4 | 4.58 | 208.81 | 58.39 | 141.78 | 317.21 |
| | 160.1 | 19.35 | 14.79 | 6.25 | 58.54 |

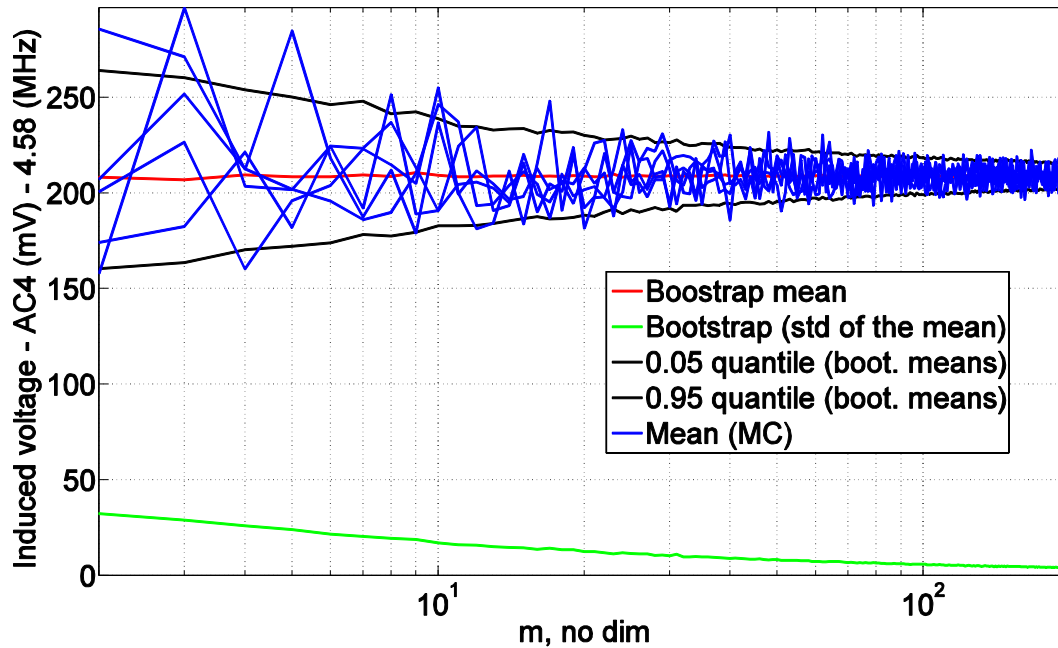


Figure 31: Mean (red), standard deviation (green) and confidence interval (black) for the bootstrapped means and 5 random Monte Carlo selections (blue) for illustration purpose in regards of the length (m) of the selected samples at 4.58 MHz.

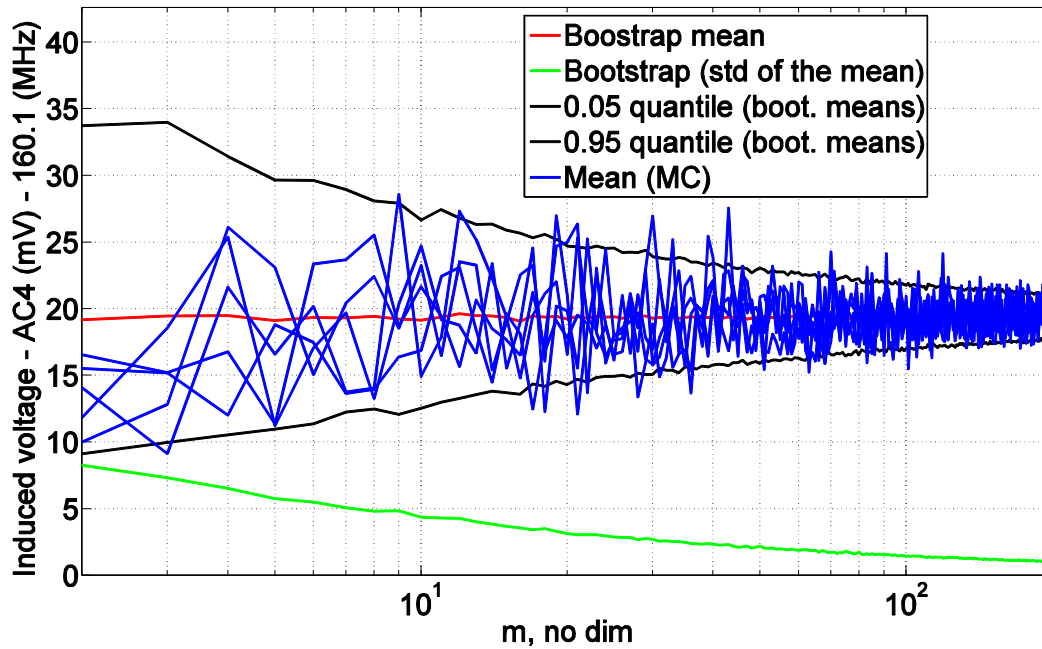


Figure 32: Mean (red), standard deviation (green) and confidence interval (black) for the bootstrapped means and 5 random Monte Carlo selections (blue) for illustration purpose in regards of the length (m) of the selected samples at 160.1 MHz.

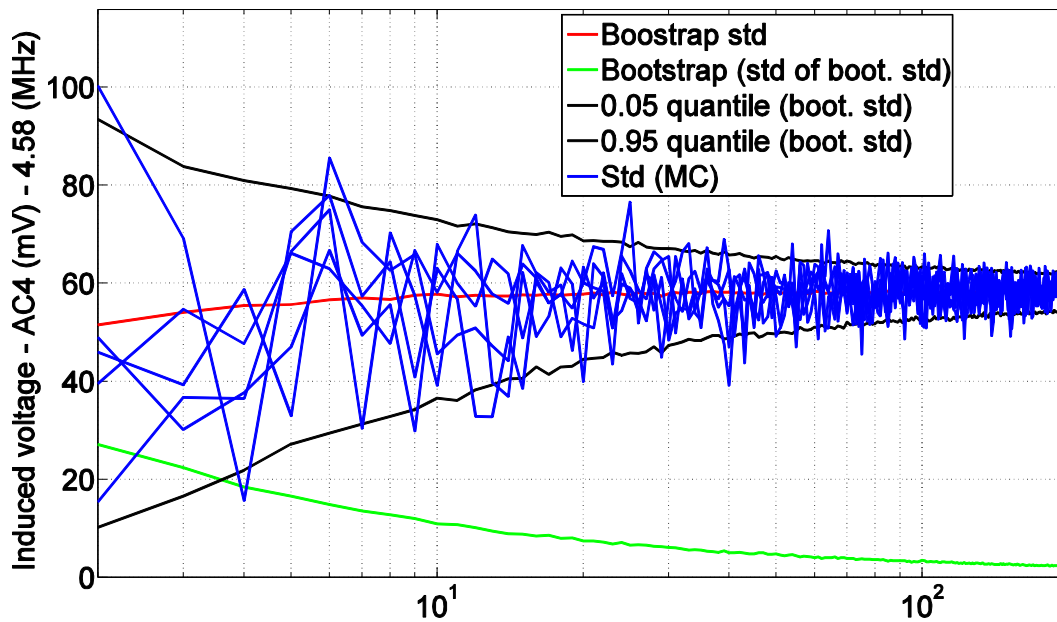


Figure 33: Mean (red), standard deviation (green) and confidence interval (black) for the bootstrapped standard deviations and 5 random Monte Carlo selections (blue) for illustration purpose in regards of the length (m) of the selected samples at 4.58 MHz.

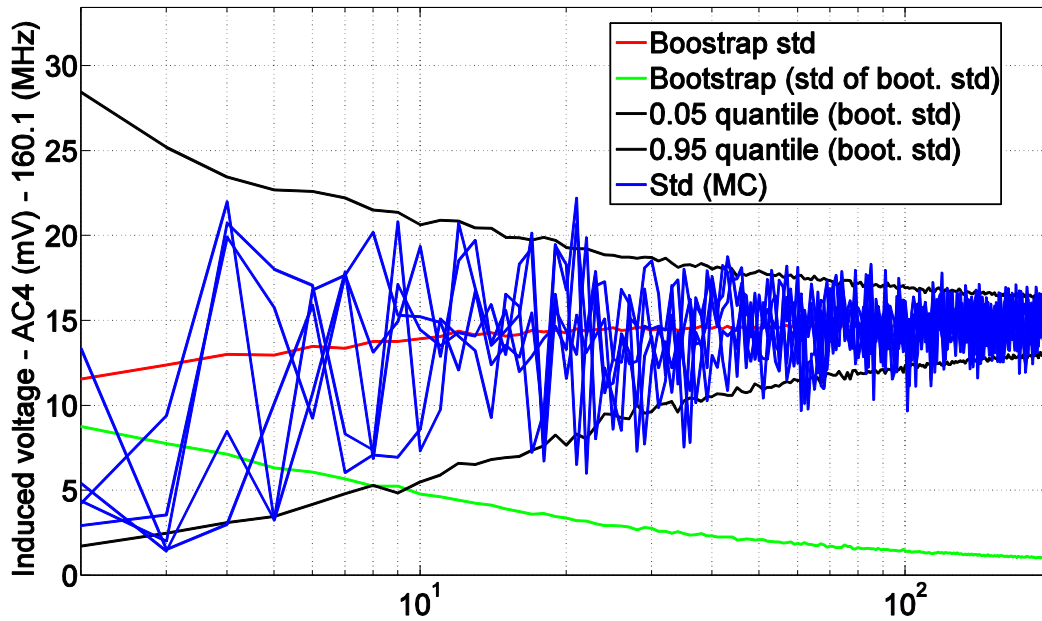


Figure 34: Mean (red), standard deviation (green) and confidence interval (black) for the bootstrapped standard deviations and 5 random Monte Carlo selections (blue) for illustration purpose in regards of the length (m) of the selected samples at 160.1 MHz.

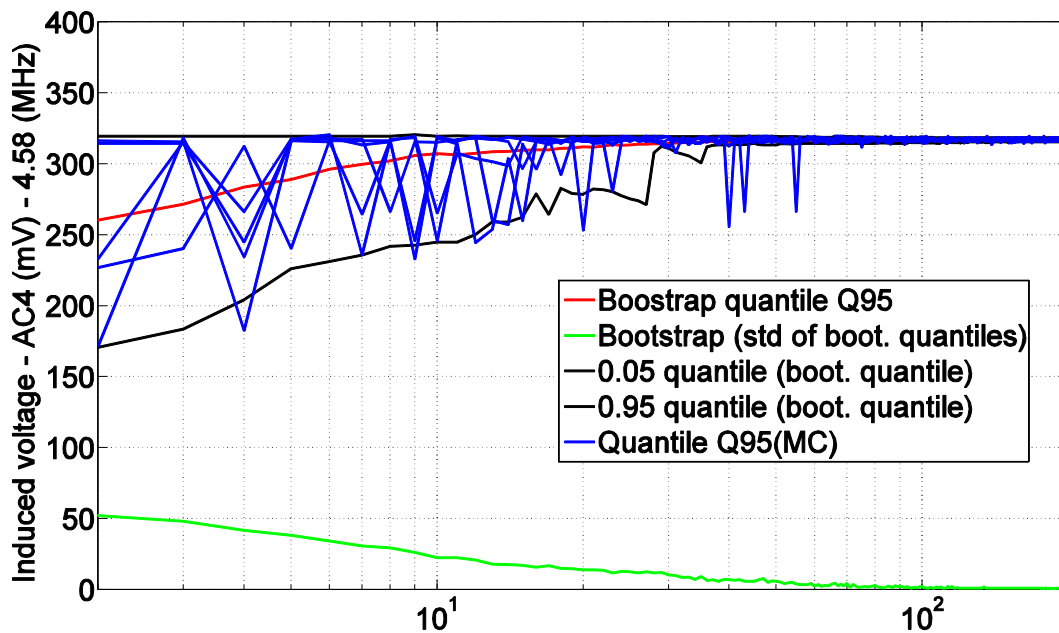


Figure 35: Mean (red), standard deviation (green) and maximum confidence interval (black) for the bootstrapped 95th- quantile (Q95) and 5 random Monte Carlo selections (blue) for illustration purpose in regards of the length (m) of the selected samples at 4.58 MHz.

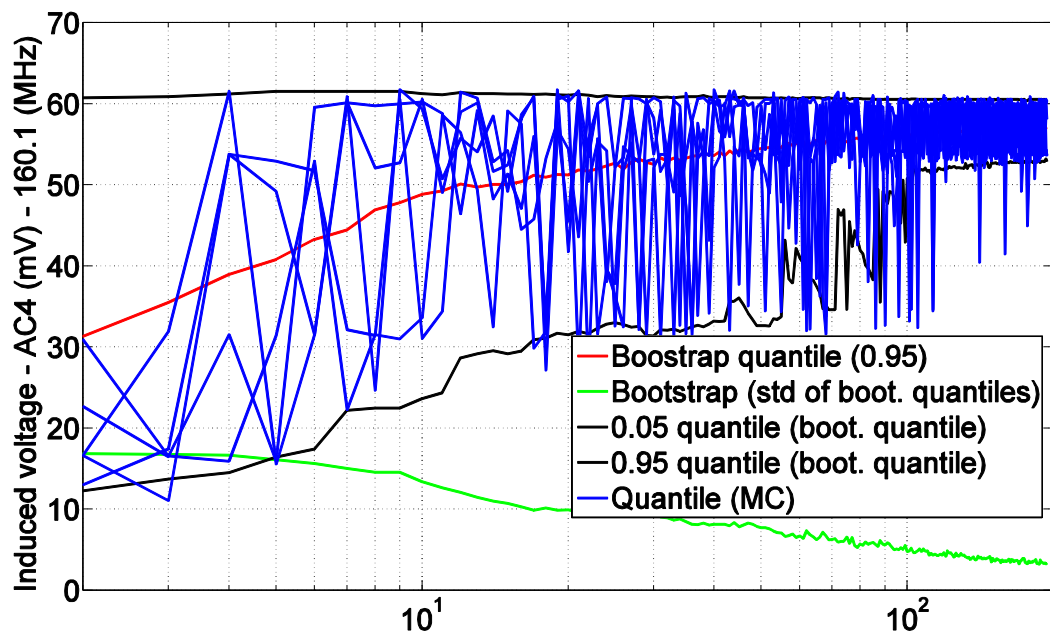


Figure 36: Mean (red), standard deviation (green) and maximum confidence interval (black) for the bootstrapped 95th- quantile (Q95) and 5 random Monte Carlo selections (blue) for illustration purpose in regards of the length (m) of the selected samples at 160.1 MHz.